

Molecular Recognition of Aqueous Dipeptides by Noncovalently Aligned Oligoglycine Units at the Air/Water Interface

Xiao Cha, Katsuhiko Ariga, Mitsuhiro Onda, and Toyoki Kunitake*[†]

Contribution from the Supramolecules Project, JRDC, 2432 Aikawa, Kurume Research Park, Kurume, 839 Japan

Received August 21, 1995[⊗]

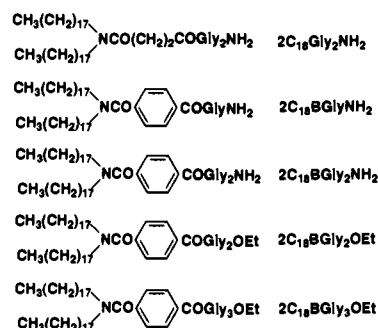
Abstract: Binding of aqueous dipeptides, GlyX and X'Gly (X = Leu, Phe, Pro, and Ala; X' = Leu and Phe), onto monolayers of dialkyl oligoglycyl amphiphiles has been investigated by π -A isotherm measurement, FT-IR spectroscopy, and XPS elemental analysis. Dipeptides with the N-terminal glycine residue (GlyX) were selectively bound onto monolayers of an amphiphile in which dioctadecylamine moiety was connected with the glycyglycinamide head group via the terephthaloyl unit. When the dipeptide (GlyLeu) concentration in the subphase was varied, the Langmuir-type saturation behavior was observed with the equimolar binding and the binding constant of 35 M^{-1} . The binding efficiency increased in the order of GlyPhe > GlyLeu > GlyPro > GlyAla, implying that the binding is promoted by hydrophobic interaction. The binding was not detected when either of the terephthaloyl and glycyglycinamide units were absent in the monolayer component. Dipeptides with the C-terminal glycine residue (X'Gly) were not bound at all. These results are satisfied by a molecular model in which guest peptides were inserted into the monolayer from the C-terminal. The observed binding selectivity is explained by hydrophobic interaction between the side chain of the C-terminal residue and the hydrophobic cavity in the monolayer and formation of stable antiparallel hydrogen bonding between guest dipeptides and host diglycine chains. The formation of a specific binding site by noncovalent self-assembly leads to a new thinking in the monolayer research.

Introduction

Astonishing variety of the peptide-peptide interaction has been demonstrated in the function of receptor proteins and antibodies.^{1,2} Efficient binding of peptide units in these cases is induced by juxtaposition of hydrogen bonding, coulombic interaction, and hydrophobic attraction between host and guest. As the details of these molecular interactions are unveiled, there began intensive efforts to design their synthetic analogs that are characterized by restricted conformational mobility and multiple interaction sites.^{3–9}

The biological receptor site is usually situated on the surface of biological supramolecular systems. Molecular monolayers at the air/water interface are convenient systems to reproduce some of the features of the biological surface. For example, we have shown that complementary hydrogen bonding act efficiently as a means of molecular recognition by functional monolayers in spite of the presence of bulk water.^{10–12}

Chart 1



In this article, we demonstrate that specific binding of dipeptides by host monolayers is feasible by proper molecular design of peptide amphiphiles. The particular compounds we chose in this study are given in Chart 1. They are dioctadecyl derivatives of oligoglycine polar moieties. The oligoglycine unit provides simple, easy-to-dissect binding sites.

We examined in our previous study¹³ the monolayer behavior of single-chain derivatives of oligoglycines. These amphiphiles formed stable molecular monolayers on water; however, probably because of strong interpeptide hydrogen bonding, they did not show detectable receptor capabilities.

Experimental Section

Synthesis of Amphiphiles. Amphiphiles $2\text{C}_{18}\text{Gly}_2\text{NH}_2$, $2\text{C}_{18}\text{BGlyNH}_2$, $2\text{C}_{18}\text{BGly}_2\text{NH}_2$, $2\text{C}_{18}\text{BGly}_2\text{OEt}$, and $2\text{C}_{18}\text{BGly}_3\text{OEt}$ were

(10) Kurihara, K.; Ohto, K.; Honda, Y.; Kunitake, T. *J. Am. Chem. Soc.* **1991**, *113*, 5077.

(11) Sasaki, D. Y.; Kurihara, K.; Kunitake, T. *J. Am. Chem. Soc.* **1991**, *113*, 9685.

(12) Sasaki, D. Y.; Kurihara, K.; Kunitake, T. *J. Am. Chem. Soc.* **1992**, *114*, 10994.

(13) Cha, X.; Ariga, K.; Kunitake, T. *Bull. Chem. Soc. Jpn.* Submitted for publication.

[†] Permanent address: Faculty of Engineering, Kyushu University, Fukuoka 812.

[⊗] Abstract published in *Advance ACS Abstracts*, November 15, 1995.

(1) E.g., Germain, R. N.; Margulies, D. H. *A. Rev. Immun.* **1994**, *11*, 403.

(2) Lauffenburger, D. A.; Linderman, J. J. *Receptors: Models for Binding, Trafficking, and Signaling*; Oxford University Press: New York, 1993; p 365.

(3) Jeong, K.-S.; Muehldorf, A. V.; Rebek, J. *J. Am. Chem. Soc.* **1990**, *112*, 6144.

(4) Hong, J. I.; Namgoong, S. K.; Bernardi, A.; Still, W. C. *J. Am. Chem. Soc.* **1991**, *113*, 5111.

(5) Borchardt, A.; Still, W. C. *J. Am. Chem. Soc.* **1994**, *116*, 373.

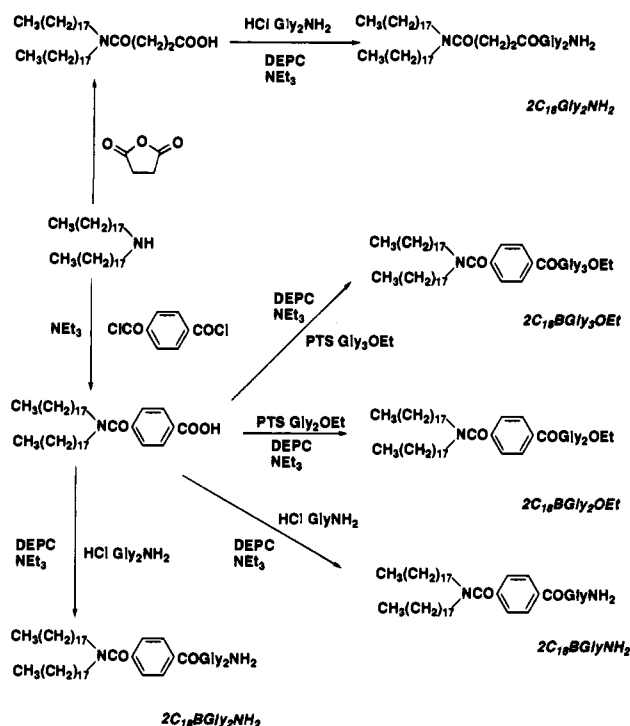
(6) Voyer, N.; Deschênes, D.; Dernier, J.; Roby, J. *J. Chem. Soc., Chem. Commun.* **1992**, 134.

(7) Tabet, M.; Labrov, V.; Sheppard, P.; Sasaki, T. *J. Am. Chem. Soc.* **1993**, *115*, 3866.

(8) Albert, J. S.; Goodman, M. S.; Hamilton, A. D. *J. Am. Chem. Soc.* **1995**, *117*, 1143.

(9) Labrenz S. R.; Kelly, J. W. *J. Am. Chem. Soc.* **1995**, *117*, 1655.

Chart 2



synthesized by the pathway given in Chart 2. Syntheses of PTS Gly₂OEt,¹³ PTS Gly₃OEt,¹³ dioctadecylamine,¹⁴ and *N,N*-dioctadecylsuccinamic acid¹⁴ were described elsewhere. The other chemicals for the lipid syntheses were commercially available. Melting points were recorded on a Yanaco micro melting point apparatus and uncorrected. Chemical shifts of ¹H NMR spectra were recorded on a Bruker ARX-300 (300 MHz) spectrometer and are given relative to chloroform (δ 7.26) or tetramethylsilane (δ 0.00). Elemental analyses (C, H, and N) were performed at Faculty of Science, Kyushu University.

2C₁₈Gly₂NH₂. *N,N*-Dioctadecylsuccinamic acid (0.500 g, 0.804 mmol) was dissolved in CH₂Cl₂ (200 mL). Diethyl phosphorocyanidate (DEPC; 0.160 mL, 1.05 mmol) was added to the solution at 0 °C. After 20 min, glycyglycinamide hydrochloride (0.192 g, 1.14 mmol) and triethylamine (0.600 mL, 4.30 mmol) dissolved in dry DMF (50 mL) was added. After a 44.5-h reaction at room temperature, the solvents were removed in vacuo. Recrystallization of the residue from acetonitrile (30 mL) gave the desired product as colorless crystals (0.487 g, 82.3%): mp 73.0–75.0 °C; ¹H NMR (CDCl₃) δ 0.88 (t, 6H, *J* = 6.7 Hz, 2 CH₃), 1.26 (br, 60H, 30 CH₂ in long chain), 1.45–1.61 (br, 4H, 2 NCH₂CH₂), 2.44 (t, 2H, *J* = 5.6 Hz, COCH₂), 2.78 (t, 2H, *J* = 5.6 Hz, COCH₂), 3.20 (t, 4H, *J* = 6.7 Hz, 2 NCH₂), 3.92 (d, 2H, *J* = 6.5 Hz, glycine CH₂), 3.94 (d, 2H, *J* = 6.2 Hz, glycine CH₂), 5.20 (br, 1H, amide H), 6.51 (br, 1H, amide H), 6.67 (br, 1H, amide H), 8.11 (br, 1H, amide H). Anal. Calcd for C₄₄H₈₆N₄O₄·³/₂H₂O: C, 69.34; H, 11.77; N, 7.35. Found: C, 69.56; H, 11.61; N, 7.53.

***N,N*-Dioctadecylterephthalamide.** Terephthaloyl chloride (1.54 g, 7.61 mmol) was dissolved in dry DMF (50 mL) and CH₂Cl₂ (100 mL). Dioctadecylamine (0.733 g, 1.40 mmol) and triethylamine (2.40 mL, 17.2 mmol) dissolved in dry DMF (50 mL) and CH₂Cl₂ (100 mL) were added to the acid chloride solution dropwise (15 min). After a 40-min reaction at room temperature, the solvents were removed in vacuo. CH₂Cl₂ was added to the residue, and the organic layer was washed with aqueous HCl twice. After the organic layer was dried over Na₂SO₄, the solvent was removed in vacuo. The residue was purified by silica gel column chromatography: *R*_f = 0.1 with hexane/EtOAc (75/25), this component also showed *R*_f = 0.6 with CHCl₃/MeOH (90/10). This purification gave the desired product as white solid (0.410 g, 43.6%): mp 41.5–42.0 °C; ¹H NMR (CDCl₃) δ 0.88 (t, 6H, *J* = 6.6 Hz, 2 CH₃), 1.25 (br, 60H, 30 CH₂), 1.48–1.65 (br,

4H, 2 NCH₂CH₂), 3.14 (t, 2H, *J* = 7.0 Hz, NCH₂), 3.49 (t, 2H, *J* = 7.4 Hz, NCH₂), 7.44 (d, 2H, *J* = 8.0 Hz, Ar H), 8.13 (d, 2H, *J* = 7.9 Hz, Ar H). Anal. Calcd for C₄₄H₇₉N₃O₃: C, 78.86; H, 11.88; N, 2.09. Found: C, 78.77; H, 11.75; N, 2.12.

2C₁₈BGlyNH₂. *N,N*-Dioctadecylterephthalamide (0.078 g, 0.12 mmol) was dissolved in CH₂Cl₂ (100 mL). DEPC (0.030 mL, 0.20 mmol) was added to the solution at 0 °C. After 20 min, glycylglycine hydrochloride (0.018 g, 0.16 mmol) and triethylamine (0.050 mL, 0.36 mmol) dissolved in dry DMF (50 mL) were added. After a 42-h reaction at room temperature, the solvents were removed in vacuo. Purification of the residue with silica gel column chromatography (CHCl₃/MeOH = 95/5, *R*_f = 0.2) gave the desired product as white solid (0.077 g, 87%): mp 34.5 (LC) → 52.5–53.5 °C; ¹H NMR (CDCl₃) δ 0.88 (t, 6H, *J* = 6.6 Hz, 2 CH₃), 1.25 (br, 60H, 30 CH₂ in long chain), 1.46–1.56 (br, 4H, 2 NCH₂CH₂), 3.11 (br, 2H, NCH₂), 3.48 (br, 2H, NCH₂), 4.17 (d, 2H, *J* = 4.9 Hz, glycine CH₂), 5.46 (br, 1H, amide H), 5.88 (br, 1H, amide H), 6.92 (br, 1H, amide H), 7.43 (d, 2H, *J* = 8.2 Hz, Ar H), 7.85 (d, 2H, *J* = 8.3 Hz, Ar H). Anal. Calcd for C₄₆H₈₃N₃O₃·¹/₂H₂O: C, 75.15; H, 11.52; N, 5.72. Found: C, 74.94; H, 11.39; N, 5.45.

2C₁₈BGly₂NH₂. *N,N*-Dioctadecylterephthalamide (0.191 g, 0.285 mmol) was dissolved in CH₂Cl₂ (200 mL). DEPC (0.070 mL, 0.46 mmol) was added to the solution at 0 °C. After 20 min, glycyglycylglycine hydrochloride (0.060 g, 0.36 mmol) and triethylamine (0.120 mL, 0.86 mmol) dissolved in dry DMF (50 mL) were added. After a 48-h reaction at room temperature, the solvents were removed in vacuo. Purification of the residue with silica gel column chromatography (CHCl₃/MeOH = 90/10, *R*_f = 0.3) gave the desired product as a white solid (0.190 g, 83.3%): mp 115.0–116.0 °C; ¹H NMR (CDCl₃) δ 0.88 (t, 6H, *J* = 6.6 Hz, 2 CH₃), 1.25 (br, 60H, 30 CH₂ in long chain), 1.47–1.68 (br, 4H, 2 NCH₂CH₂), 3.13 (br, 2H, NCH₂), 3.46 (br, 2H, NCH₂), 3.75 (br, 2H, glycine CH₂), 4.03 (br, 2H, glycine CH₂), 5.93 (br, 2H, amide H), 6.71 (br, 1H, amide H), 7.37 (d, 2H, *J* = 8.1 Hz, Ar H), 7.86 (d, 2H, *J* = 8.1 Hz, Ar H), 7.93 (br, 1H, amide H). Anal. Calcd for C₄₈H₈₆N₄O₄·H₂O: C, 71.95; H, 11.07; N, 6.99. Found: C, 71.89; H, 11.02; N, 6.82.

2C₁₈BGly₂OEt. *N,N*-Dioctadecylterephthalamide (0.199 g, 0.297 mmol) was dissolved in CH₂Cl₂ (100 mL). DEPC (0.100 mL, 0.66 mmol) was added to the solution at 0 °C. After 20 min, PTS Gly₂OEt (0.106 g, 0.319 mmol) and triethylamine (0.150 mL, 1.08 mmol) dissolved in CH₂Cl₂ (50 mL) were added. After a 72-h reaction at room temperature, the organic layer was washed with water and dried over Na₂SO₄. After the solvent was removed in vacuo, recrystallization of the residue from acetonitrile (50 mL) gave the desired product as a white solid (0.192 g, 79.7%): mp 65.5–66.0 °C; ¹H NMR (CDCl₃) δ 0.88 (t, 6H, *J* = 6.6 Hz, 2 CH₃ in long chain), 1.25 (br, 60H, 30 CH₂ in long chain), 1.29 (t, 3H, *J* = 7.2 Hz, COOCH₂CH₃), 1.47–1.57 (br, 4H, 2 NCH₂CH₂), 3.13 (br, 2H, NCH₂), 3.48 (br, 2H, NCH₂), 4.09 (d, 2H, *J* = 5.1 Hz, glycine CH₂), 4.20 (d, 2H, *J* = 5.1 Hz, glycine CH₂), 4.23 (q, 2H, *J* = 7.1 Hz, 2H, COOCH₂), 6.46 (br, 1H, amide H), 6.94 (br, 1H, amide H), 7.42 (d, 2H, *J* = 8.2 Hz, Ar H), 7.85 (d, 2H, *J* = 8.2 Hz, Ar H). Anal. Calcd for C₅₀H₈₉N₃O₅·¹/₄H₂O: C, 73.53; H, 11.04; N, 5.14. Found: C, 73.50; H, 11.03; N, 5.10.

2C₁₈BGly₃OEt. *N,N*-Dioctadecylterephthalamide (0.085 g, 0.13 mmol) was dissolved in CH₂Cl₂ (100 mL). DEPC (0.030 mL, 0.20 mmol) was added to the solution at 0 °C. After 20 min, PTS Gly₃OEt (0.063 g, 0.16 mmol) and triethylamine (0.060 mL, 0.43 mmol) dissolved in CH₂Cl₂ (50 mL) were added. After a 50-h reaction at room temperature, the organic layer was washed with water and dried over Na₂SO₄. After the solvent was removed in vacuo, purification of the residue with silica gel column chromatography (CHCl₃/MeOH = 95/5, *R*_f = 0.6) gave the desired product as white solid (0.090 g, 82%): mp 110.5–111.0 °C; ¹H NMR (CDCl₃) δ 0.88 (t, 6H, *J* = 6.6 Hz, 2 CH₃ in long chain), 1.26 (br, 60H, 30 CH₂ in long chain), 1.27 (t, 3H, *J* = 7.3 Hz, COOCH₂CH₃), 1.47–1.66 (br, 4H, 2 NCH₂CH₂), 3.13 (br, 2H, NCH₂), 3.47 (br, 2H, NCH₂), 3.93 (d, 2H, *J* = 5.3 Hz, glycine CH₂), 4.02 (d, 2H, *J* = 5.3 Hz, glycine CH₂), 4.05 (d, 2H, *J* = 5.1 Hz, glycine CH₂), 4.19 (q, 2H, *J* = 7.2 Hz, COOCH₂), 6.96 (br, 1H, amide H), 7.06 (br, 1H, amide H), 7.40 (d, 2H, *J* = 8.0 Hz, Ar H), 7.50 (br, 1H, amide H), 7.87 (d, 2H, *J* = 8.0 Hz, Ar H). Anal. Calcd for C₅₂H₉₂N₄O₆: C, 71.85; H, 10.67; N, 6.44. Found: C, 71.53; H, 10.65; N, 6.28.

(14) The details of these syntheses will be presented in a forthcoming publication, Onda, M.; Yoshihara, K.; Koyano, H.; Ariga, K.; Kunitake T. Manuscript in preparation.

Surface Pressure-Area (π -A) Isotherms. A computer-controlled film balance system FSD-110 (trough size, 100 \times 200 mm, USI System, Japan) was used. π -A Isotherms were taken at a compression rate of 4 $\text{mm}\cdot\text{min}^{-1}$ and a subphase temperature of 20.0 ± 0.3 $^{\circ}\text{C}$. The subphase water was deionized and doubly distilled. The spreading solutions of oligoglycine amphiphiles were ca. 0.16 $\text{mg}\cdot\text{cm}^{-3}$ in CHCl_3 .

LB Films. A gold-deposited slide glass was used as a substrate for LB transfer in order to measure reflection-absorption FT-IR spectra. It was prepared as follows. Slide glass (pre-cleaned, 176 \times 26 \times 1 mm, Iwaki Glass) was immersed in a detergent solution overnight (Dsn90, Bokusui Brown Co. Ltd.). The glass was washed with a large excess of ion-exchanged water to remove the detergent completely and subjected to sonication in fresh ion-exchanged water several times. After the glass was dried under vacuum over 1 h, chromium and gold thin layers were consecutively formed by the vapor-deposition method (500 Å Au/50 Å Cr/slide glass) with a vapor-deposition apparatus VPC-260 (ULVAC Kyushu).

Monolayers were transferred onto gold-deposited glass slides in the vertical mode at a surface pressure of 20 $\text{mN}\cdot\text{m}^{-1}$ and at upstroke and downstroke motions of 8 and 100 $\text{mm}\cdot\text{min}^{-1}$, respectively, from pure water and dipeptide subphases. The transfer ratio was 1.0 ± 0.1 in the upstroke mode, but there was no transfer in the downstroke mode for amphiphile 1, 3, and 5, and it was 1.0 ± 0.1 in the upstroke mode and $0.2\text{--}0.4 \pm 0.1$ in the downstroke mode for amphiphile 2 and 4.

FT-IR Measurements. Infrared spectra of the LB film on gold-deposited glass were obtained on an FT-IR spectrometer (Nicolet 710) equipped with a MCT detector (for RAS, reflection absorption spectroscopy). All data were collected by the RAS method at a spectral resolution of 4 cm^{-1} .

XPS Measurement. X-ray photoelectron spectra of the LB films on gold-deposited glass were measured with a Perkin-Elmer PHI 5300 ESCA instrument: (X-ray source $\text{MgK}\alpha$ 300 W, scan range 0–1000 eV, takeoff angle 45°). The elemental composition was obtained by dividing the observed peak area by intrinsic sensitivity factors of each element.

Results and Discussion

Monolayer Behavior and Langmuir-Blodgett Transfer.

A π -A isotherm of $2\text{C}_{18}\text{Gly}_2\text{NH}_2$ showed a condensed phase only with a limiting molecular area of 0.5 nm^2 and a collapse pressure of 56 $\text{mN}\cdot\text{m}^{-1}$ (data not shown). It appears that the monolayer is highly crystallized even at low surface pressures. It was difficult to transfer this monolayer onto solid substrates either from the pure water subphase or from dipeptide guest solutions. In order to improve the transfer property, we subsequently synthesized double-chain oligoglycine amphiphiles that additionally possess the benzene ring between the nonpolar and polar moieties. The four oligoglycine derivatives of this kind as listed in Chart 1 showed π -A curves with expanded phases at low pressures on pure water and on aqueous dipeptide subphases. These monolayers have limiting areas of ca. 0.5 nm^2 and collapse pressures at 46–56 $\text{mN}\cdot\text{m}^{-1}$. As examples, π -A curves of $2\text{C}_{18}\text{BGly}_2\text{NH}_2$ monolayer on different subphases are shown in Figure 1. On pure water it gave a limiting molecular area of 0.52 nm^2 and collapse pressure of 48 $\text{mN}\cdot\text{m}^{-1}$. The π -A curve on subphase of 0.01 M GlyLeu was a little more expanded than that on pure water, giving a limiting area of 0.57 nm^2 and an unchanged collapse pressure of 48 $\text{mN}\cdot\text{m}^{-1}$. On 0.05 M GlyLeu, the π -A curve was more expanded and gave a limiting area of 0.67 nm^2 and a collapse pressure of 47 $\text{mN}\cdot\text{m}^{-1}$. These monolayers are easily transferred onto quartz or gold-deposited glass plates at a subphase pressure of 25 $\text{mN}\cdot\text{m}^{-1}$.

Dipeptide Binding Capability. In the initial stage, we tested binding of GlyLeu, GlyPhe, and $(\text{Gly})_3$ with the latter four peptide monolayers by measuring FT-IR spectra of transferred LB films. Characteristic IR peaks of these peptides were not essentially detected except for the monolayer of $2\text{C}_{18}\text{BGly}_2$ -

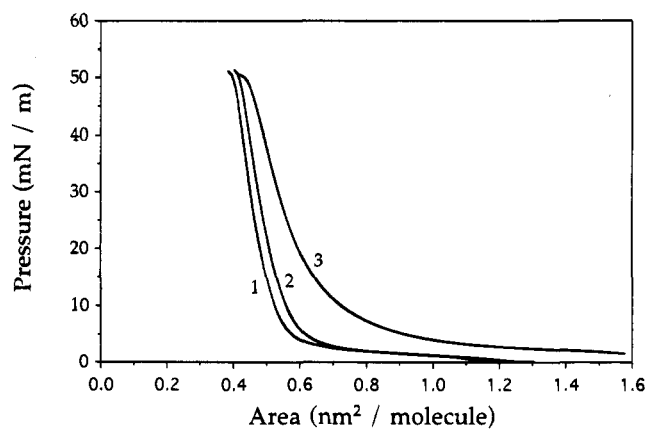


Figure 1. π -A isotherms of $2\text{C}_{18}\text{BGly}_2\text{NH}_2$ monolayers at 20.0 ± 0.3 $^{\circ}\text{C}$ (1) on pure water, (2) on 0.01 M GlyLeu, (3) on 0.05 M GlyLeu.

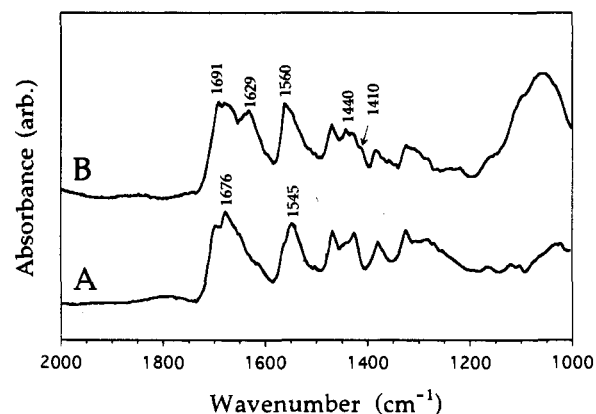


Figure 2. FTIR-RAS spectra of LB films of $2\text{C}_{18}\text{BGly}_2\text{NH}_2$ monolayers (15 layers) transferred from pure water (A), and from 0.01 M GlyLeu (B).

NH_2 , although a trace amount of GlyPhe appeared to be bound to $2\text{C}_{18}\text{BGly}_3\text{OEt}$. An LB film (14 layers) of $2\text{C}_{18}\text{BGly}_2\text{NH}_2/\text{GlyLeu}$ shows characteristic IR peaks for the guest dipeptide at 1691 ($\text{N}_\text{C}=\text{O}$ (COOH)), 1629 (amide I), 1560 (amide II), 1440 (δ_{CH_3} , deformation), and 1410 (Δ_{COO^-}) cm^{-1} , in addition to amide I (1676 cm^{-1}) and amide II (1545 cm^{-1}) bands of the host monolayer (Figure 2).

The superior receptor property of the $2\text{C}_{18}\text{BGly}_2\text{NH}_2$ monolayer was subsequently examined for a larger variety of dipeptides by means of X-ray photoelectron spectroscopy (XPS). The amount of guest dipeptides that accompanied the LB film of $2\text{C}_{18}\text{BGly}_2\text{NH}_2$ was determined on the basis of the C/N ratio in the XPS analysis. For example, the LB film transferred from 10 and 40 mM of aqueous GlyLeu showed smaller C/N values (10.9 and 9.6, respectively) than that of the film transferred from pure water (C/N = 12.0). These values were converted to 0.33 and 0.85 of guest/host ratios, respectively, with correction upon the structural factor. Figure 3 compares the extent of dipeptide incorporation from their 0.01 M solutions. It is clear that some dipeptides are specifically bound: GlyX dipeptides (X: Leu, Phe, Pro, and Ala) are bound, but X'Gly (X': Leu and Phe) are not. The other dipeptides (HisLeu, AlaAla, and LeuLeu) are not detectably bound under the same experimental conditions. The IR data of transferred films were consistent with the XPS results. In the presence of 0.01 M GlyGly in the subphase, the $2\text{C}_{18}\text{BGly}_2\text{NH}_2$ monolayer that was deposited in the upstroke motion was again dissolved in the subphase in the downstroke motion. We could not determine the binding efficiency of GlyGly because of a poor reproducibility in XPS measurement on the single monolayer film. However, $2\text{C}_{18}\text{BGly}_2\text{NH}_2$ mono-

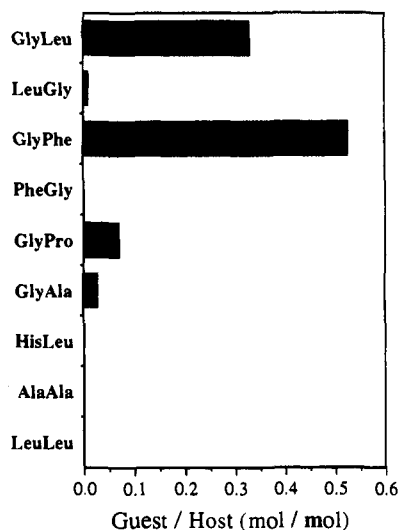


Figure 3. Binding ratio (guest/host) of different aqueous dipeptides by $2C_{18}BGly_2NH_2$ monolayer, as determined from XPS spectra of transferred LB films (15 layers). Concentrations in subphases are 0.01 M.

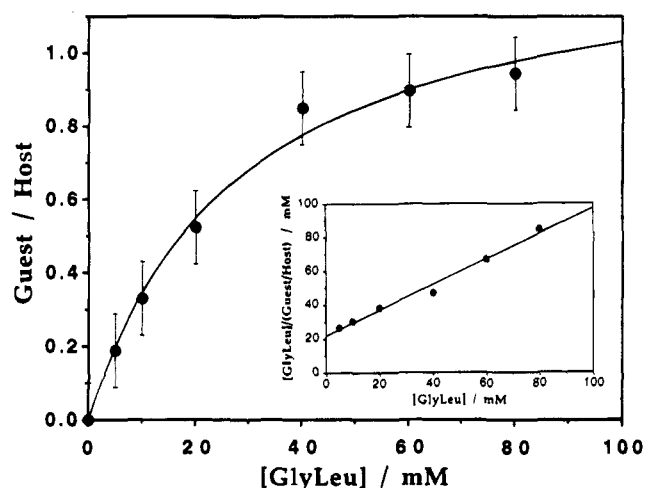


Figure 4. Binding of aqueous GlyLeu to $2C_{18}BGly_2NH_2$ monolayer at 20 °C, and its analysis by the Langmuir isotherm.

layer was transferred from 0.01 M GlyGlyGly, and XPS results indicated the host/guest ratio of 6:1.

The binding behavior of GlyLeu was examined more closely as shown in Figure 4. As the concentration of GlyLeu guest increases, the guest/host ratio increases and reaches equimolar saturation at ca. 50 mM. The plots were analyzed by using the Langmuir isotherm,

$$[S]/y = 1/(\alpha K) + [S]/\alpha \quad (1)$$

where y is the guest/host ratio at saturation, $[S]$ is the guest concentration in the subphase, α is saturation binding ratio, and K is binding constant. The linear relation derived from experimental data gives a site occupancy (i.e., the guest/host ratio at saturation) of 1.3 and a binding constant of 35 M^{-1} . The site occupancy may be regarded as unity, when experimental errors are considered. We can conclude that GlyLeu molecules are bound to the monolayer in the equimolar ratio.

Nature of Receptor Site. The mechanism of dipeptide binding can be inferred from IR spectroscopy study. FTIR-RAS spectra of LB films of $2C_{18}BGly_2NH_2$ that are transferred from 0.04–0.08 M aqueous GlyLeu (80–90% binding saturation) contain very strong characteristic peaks of GlyLeu (1686 ($\nu_{C=O}$ (COOH)), 1629 (amide I), 1561 (amide II), 1450 (δ_{CH_3}),

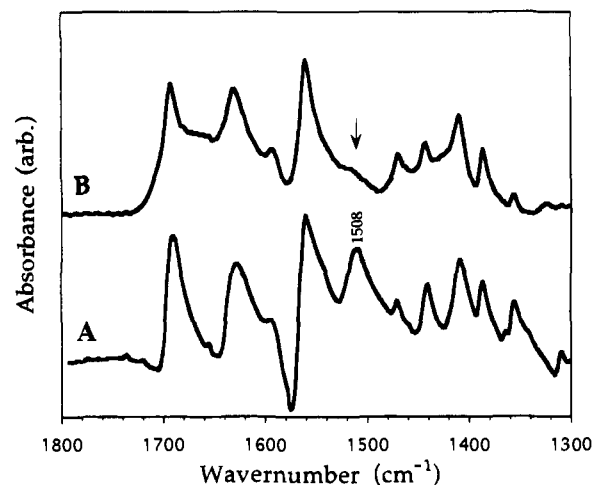


Figure 5. FTIR-RAS spectra of a GlyLeu film cast from $H_2O/MeOH$ solution (A) and a LB film of $2C_{18}BGly_2NH_2$ monolayers (15 layers) transferred from 0.04 M GlyLeu (B).

and 1410 cm^{-1} (Δ_{COO^-}), see Figure 5B). An obvious difference from that of a cast film of the guest molecule (Figure 5A) is the absence of the $\delta_{NH_3^+}$ (deformation) peak of GlyLeu at 1508 cm^{-1} (see arrow in Figure 5B). This suggests that the terminal NH_3^+ group is strongly hydrogen bonded to proton receptors. This band may also disappear when a salt bridge is formed. But this is unlikely since the anionic moiety is not contained in the monolayer. The ν_{NH} peak of the host/guest LB film is located at around 3270 cm^{-1} . Although it is not clear whether this peak is composed of an overlap of NH peaks of the host monolayer (3309 cm^{-1}) and guest GlyLeu (3232 cm^{-1}) or is a new one derived from interaction between the guest and the host, we cannot deny that the major fraction of the amide NH unit in the host and guest molecules is engaged in hydrogen bonding.¹⁵

In our previous study,¹³ a series of octadecyl-derivatized oligoglycine amphiphiles, $C_{18}Gly_nOEt$ ($n = 1-5$), formed relatively stable monolayers with condensed phases alone and did not show detectable peptide-binding ability. IR spectroscopic study revealed that these monolayers consisted either of the amide NH unit with rather strong intermolecular hydrogen bonding (ν_{NH} at 3294 to 3299 cm^{-1} for $C_{18}Gly_nOEt$ ($n = 3, 4$, and 5)), of amide NH of strong and weak hydrogen bonds (ν_{NH} at 3322 and 3270 cm^{-1} for $C_{18}Gly_2OEt$), or of relatively free NH units (ν_{NH} 3311 cm^{-1} for $C_{18}GlyOEt$). The lack of dipeptide binding for these single-chain amphiphiles was attributed to saturated hydrogen bonding in the case of the longer oligoglycine units, as suggested by lower frequencies of the ν_{NH} band. In the case of shorter glycine units (Gly and Gly₂), the amide NH was at least partially free of interpeptide hydrogen bonding, but apparently the number of the amide site was not sufficient for effective binding.

Figure 6 shows schematic illustrations of the packing mode in monolayers of single alkyl and double alkyl components and the arrangement of bound guest molecules. The limiting molecular area of the single-chain oligoglycine amphiphile is $0.29-0.30 \text{ nm}^2$. This is larger than the molecular cross section of the methylene chain (0.2 nm^2) and indicates tilted alkyl packing of the single-chain amphiphiles. The average distance of the neighboring glycine residues is about 0.5 nm , and, as discussed above, IR data show partial formation of intermolecular hydrogen bonds. The guest dipeptide (for example, approximate molecular cross section is about $0.18-0.19 \text{ nm}^2$

(15) Bellamy, L. J. *The Infrared Spectra of Complex Molecules*, 3rd ed.; Chapman and Hall Ltd: London, 1975; Vol. 1, p 233.

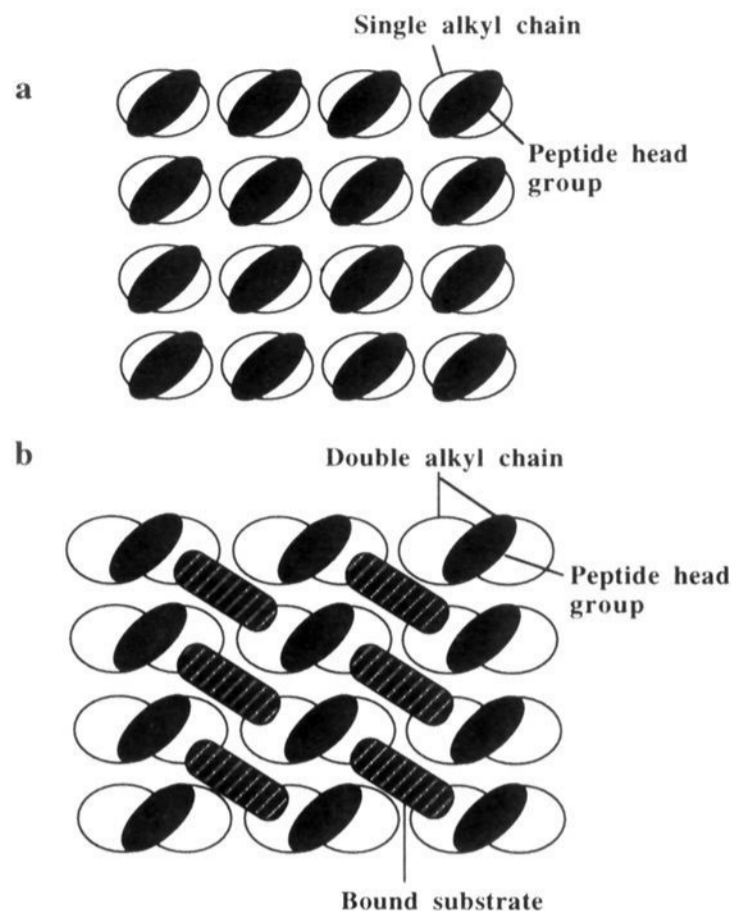


Figure 6. Packing patterns in monolayers of (a) single alkyl oligoglycine amphiphiles and (b) double alkyl oligoglycine amphiphiles (with bound guest dipeptides). Projection from bottom.

even for the smallest GlyGly) would be hardly accommodated into the intermolecular cavity even if it is available (Figure 6a).

In the case of double-chain oligoglycine derivatives, it is assumed that the enlarged cross section of the alkyl chain portion separates the oligoglycine terminals to create peptide binding cavities. The ν_{NH} peak positions are in fact shifted to higher frequencies (3300–3330 cm^{-1}), indicating weakened intermolecular hydrogen bonds. This supposition was endorsed by efficient binding of GlyLeu to the $2\text{C}_{18}\text{BGly}_2\text{NH}_2$ monolayer. The observed equimolar binding may be schematically represented by Figure 6b. The ν_{NH} peak of this monolayer is not unique compared with other monolayers of the double-chain amphiphile that do not display binding capability toward dipeptide substrates. Therefore, the weakened intermolecular hydrogen bonding is not the sufficient condition for dipeptide binding.

Substrate Specificity. The nature of the receptor site of the $2\text{C}_{18}\text{BGly}_2\text{NH}_2$ monolayer can be inferred more closely by considering guest specificity. As summarized in Figure 3, GlyX type dipeptides were more or less bound to this monolayer, while X'Gly dipeptides were not. The binding is promoted when the N-terminal peptide unit is glycine. The limiting molecular area of this monolayer as estimated from the π -A isotherms is 0.67 nm^2 when GlyLeu is bound in 1:1 ratio. The oligoglycine moiety of the monolayer has an approximate area of 0.19 nm^2 when 3_1 -helix or β -sheet conformations are assumed. Because the monolayer was transferred at a surface pressure of 25 $\text{mN}\cdot\text{m}^{-1}$ that corresponds to a packing molecular area of 0.57 nm^2 for each host molecule, a receptor site that is surrounded by the host diglycyl units and benzene moieties would be able to accommodate a guest molecule with a cross section of about 0.38 nm^2 . It is clear that either N-terminal or C-terminal Gly unit (cross section is about 0.18–0.19 nm^2) can be easily inserted in the receptor site and form hydrogen bonds with host molecules. However, the lack of binding of XGly dipeptides suggests to us that the binding is favored only when N-terminal Gly unit is surrounded by the host diglycyl units.

The binding efficiency increased in the order of GlyPhe > GlyLeu > GlyPro > GlyAla, implying that the binding is

favored by enhanced hydrophobicity. The hydrophobicity parameter, $\log P$, of peptides can be estimated by the method of Akamatsu and Fujita,^{16,17} as follows: $\log P = -2.37$ for GlyPhe, -2.70 for GlyLeu, -3.18 for GlyPro, -3.81 for GlyAla, and -4.07 for GlyGly. These empirical estimates are in agreement with the observed order of binding and indicate that hydrophobicity of the second amino acid residue facilitates the binding.

Plausible models of incorporation of aqueous GlyPhe to a receptor site of $2\text{C}_{18}\text{BGly}_2\text{NH}_2$ monolayer are depicted in Figure 7. An optimization of amphiphile conformation¹⁸ suggests that these two alkyl chains are placed perpendicular to the benzene plane (rather than parallel to it), as shown in this figure. Figure 7a describes that a guest dipeptide (GlyPhe) is inserted into the receptor site from the C-terminal with the hydrophobic side chain of the Phe residue being laid between the benzene planes of the host molecule. The two terminals and the amide groups of the guest peptide apparently form two pairs of antiparallel hydrogen bonds with diglycyl units of the host molecule. The hydrophobic side chain of the second amino acid residue can be stably accommodated in this scheme, consistent with the observed dipeptide specificity. The cooperative effect of hydrophobic packing and hydrogen bonding would enhance substrate binding. The hydrophobic side chain of PheGly dipeptide cannot be accommodated snugly in this binding model. An alternative binding model is shown in Figure 7b. In this case, GlyPhe dipeptide is inserted into the receptor site from N-terminal glycine and forms parallel hydrogen bonds with the host monolayer. The hydrophobic side chain of Phe must be exposed to bulk water phase. This substrate arrangement is less favorable than the alternate mode of incorporation. On the other hand, the N-terminal insertion of PheGly, if it occurs, should provide a binding mode similar to C-terminal insertion of GlyPhe of Figure 7a, since the hydrophobic side chain of PheGly can be placed in the hydrophobic pocket of the host molecule. A major difference in the interaction energy between these two types of binding is the mode of hydrogen bonding. The hydrogen bonding between GlyPhe (C-terminal insertion) and the host peptide chain is in the antiparallel motif, while that between PheGly (N-terminal insertion) and the host peptide chain is parallel. It is known that hydrogen bonding between the parallel peptide chains cannot be extended linearly, and energy calculations show that the parallel interpeptide hydrogen bonding is not as stable as its antiparallel cousin.¹⁹ This structural difference may be responsible for the remarkable difference in binding behavior between GlyPhe and PheGly. Although the exact conformation of guest dipeptides bound by the monolayer is not clear, the diglycyl moiety of the monolayer, in our case, may act as a template²⁰ to induce conformational fixation of short guest peptides at the interface, resulting in antiparallel hydrogen bonding between GlyX dipeptides and the host monolayer.

As a yet other possibility, dipeptide substrates may be bound perpendicular to the host peptide chain. This is, however, unlikely, since an elongated cavity with a definite shape and size is difficult to conceive.

(16) Asao, M.; Iwamura, H.; Akamatsu, M.; Fujita, T. *J. Med. Chem.* **1987**, *30*, 1873.

(17) Akamatsu, M.; Okutani, S.; Nakao, K.; Hong, N. J.; T. Fujita, T. *Quant. Struct.-Act. Relat.* **1990**, *9*, 189.

(18) The optimum conformation was searched for its short-chain analog by using the molecular modeling program, CSC Chem 3D Plus (version 3.1.2).

(19) Walton, A. G. *Polypeptides and Protein Structure*; Elsevier North Holland, Inc: New York, 1981; p 36.

(20) Kemp, D. S.; Allen, T.; Oslick, S. *J. Am. Chem. Soc.* **1995**, *117*, 6641.

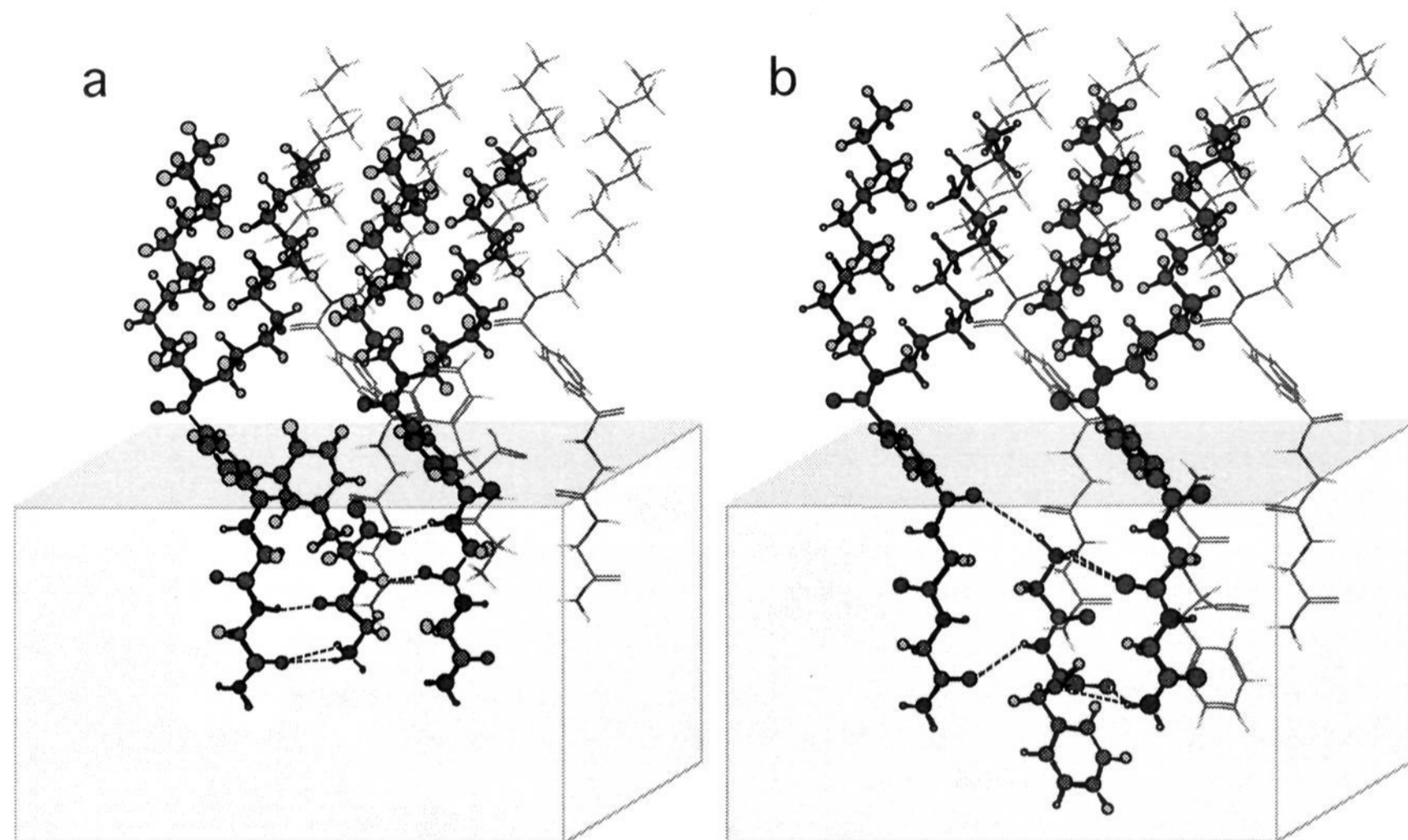


Figure 7. A conceivable pattern of hydrogen bonding interaction between $2C_{18}BGly_2NH_2$ monolayer and GlyPhe dipeptide. The guest peptide of GlyPhe is inserted into the monolayer from (a) C-terminal and (b) N-terminal. Dotted lines show hydrogen bonds.

Conclusion

The present finding clearly establishes that specific peptide binding sites can be created by self-assembly of an oligoglycine amphiphile at the air/water interface. Unexpected structural specificity on both sides of the monolayer component and the guest dipeptide is noteworthy. The presence of the benzene unit between the double alkyl chain and the diglycine unit was essential for formation of the receptor capability. Dipeptides with the N-terminal glycine residue were selectively bound to these receptor sites. It has been suspected that the noncovalent assembly in monolayers is not suitable for such purposes. Our

results prove that this is not the case. The conformational fixation of the monolayer component and the regular component arrangement due to intermolecular interaction would give rise to specific receptor sites at the air/water interface. It is clear that interplay of hydrogen bonding and hydrophobic interaction is essential for effective binding.

Since the binding site is self-assembled from individual peptide chains, we may expect to obtain a variety of binding sites by induced assembly of different component amphiphiles. Our efforts in this direction will be reported shortly.

JA952877H